



ELSEVIER

Thermochimica Acta 286 (1996) 375–386

thermochimica
acta

The effect of the addition of ZrSiO_4 on the crystallization of $30\text{Li}_2\text{O}/70\text{SiO}_2$ powdered glass

A.P. Novaes de Oliveira *, A. Bonamartini Corradi, L. Barbieri,
C. Leonelli, T. Manfredini

Department of Chemistry, Faculty of Engineering, University of Modena, Via Campi 183, 41100 Modena, Italy

Received 4 January 1996; accepted 29 January 1996

Abstract

The effects of the addition of ZrSiO_4 to $30\text{Li}_2\text{O}/70\text{SiO}_2$ powdered glass on its crystallization behaviour were investigated by means of differential thermal analysis (DTA), X-ray diffraction (XRD) and scanning electron microscopy (SEM). Transparent glasses with a ZrSiO_4 content of up to 10.30 mol% were obtained. $\text{Li}_2\text{Si}_2\text{O}_5$ and/or ZrSiO_4 , $\text{Li}_2\text{Si}_2\text{O}_5$ and tridymite were crystallized after appropriate heat treatments. Kinetics parameters for surface crystallization were estimated from the DTA curves. The crystallization was completed in the 590–907°C temperature range for activation energy values between 460.5 and 715.9 kJ mol^{-1} . The resulting materials are potential candidates for useful sintered glass-ceramics with a wide number of applications.

Keywords: Crystallization; Glass/glass-ceramics; Kinetics of crystallization; $\text{Li}_2\text{O}-\text{ZrO}_2-\text{SiO}_2$ glasses; ZrSiO_4 glasses

1. Introduction

Of the two-component alkali silicate glasses, the lithia-silica system is the most important for the preparation of glass-ceramic materials [1–3]. In the $\text{Li}_2\text{O}-\text{SiO}_2$ phase diagram, it is very important to note that an addition of approximately 30 mol% of Li_2O to SiO_2 causes the liquidus temperature to drop rapidly from 1713 to 1030°C, such that the resulting liquid forms a clear glass on cooling which is very easy to obtain. However, liquids containing less than 25 mol% Li_2O give opalescent or opaque glass on cooling owing to phase separation within a metastable immiscibility dome [1,2]. On crystallization between the glass transition temperature, approx. 500°C, and the

* Corresponding author.

solidus temperature, i.e. the melting temperature, 1030°C, $\text{Li}_2\text{Si}_2\text{O}_5$ is the main product together with small amounts of either SiO_2 and/or Li_2SiO_3 [1–3]. Usually, in order to produce a fine-grained lithium silicate glass-ceramic, the two-stage crystallization would typically involve nucleation at 450–500°C followed by growth of the $\text{Li}_2\text{Si}_2\text{O}_5$ crystals at 650–700°C [2–4], and nucleating catalysts, such as metal oxides (TiO_2 or P_2O_5), can generally be added.

However, this simple system alone shows poor properties as regards chemical durability and mechanical characteristics. Addition of oxides acting as network former and modifier can greatly improve these properties and enable glass-ceramics to be obtained with very high thermal shock resistance and surface hardness, and low coefficients of conductivity and thermal expansion.

Zircon (ZrSiO_4)-containing ceramics have become of interest because this is a crystalline phase with many unique properties. Zircon has a very low coefficient of heat and conductivity, and a low coefficient of thermal expansion [5]. Its mechanical strength does not degrade even at temperatures higher than 1400°C, and it has a thermal shock resistance superior to ceramics containing mullite and alumina [5]. The hardness of zircon on the mineralogical Mohs scale is 7.5, between quartz and topaz [5], and it has a very high refractive index with a positive birefringence. Chemically, zircon is very stable, especially at lower temperatures, and with respect to acids zircon is one of the most resistant materials [5]. In particular, the relative stability of zircon can be seen from the fact that lithia-rich silica glasses can dissolve zircon as a monomolecular substance, without association or dissociation [5].

All these properties give zircon-containing ceramics considerable potential, especially when hardness, refractive index, and chemical durability are the main requisites. To determine the maximum amount of ZrSiO_4 that can solubilize in $30\text{Li}_2\text{O}/70\text{SiO}_2$ and the possibility of obtaining $\text{Li}_2\text{O}/\text{SiO}_2$ glass-ceramics containing the largest possible amounts of ZrSiO_4 , this study reports the effect of zircon addition on the crystallization kinetics of $30\text{Li}_2\text{O}/70\text{SiO}_2$ composition powdered glass using differential thermal analysis (DTA), X-ray diffraction (XRD) and scanning electron microscopy (SEM).

2. Experimental procedure

2.1. Glass preparation

Seven compositions were prepared with additions of ZrSiO_4 of up to 11.10 mol% (Table 1). For all compositions, high-purity Li_2CO_3 , SiO_2 , and ZrSiO_4 were used as raw materials. Glasses were obtained by melting the raw materials in a Pt crucible, using a laboratory electric furnace, with a holding time of 30 min at 1400°C, and then quenching in a steel mould. Subsequently, the glasses were ground to a fine powder in an agate ball mill for 40 min to reach a grain size lower than 45 μm .

2.2. Differential thermal analysis (DTA)

Differential thermal analysis (DTA) was used to study the devitrification process in amorphous glasses. To measure the typical temperatures (T_g , T_c , and T_m) of

Table 1
Composition of the glasses studied

Glass composition	Constituent/mol%			Yield
	Li ₂ O	SiO ₂	ZrSiO ₄	
GC-0	30.00	70.00	–	Clear glass
GC-1	29.30	68.30	2.40	Clear glass
GC-2	28.60	66.60	4.80	Clear glass
GC-3	27.90	65.10	7.00	Clear glass
GC-4	27.30	63.60	9.10	Clear glass
GC-5	26.90	62.80	10.30	Clear glass
GC-6	26.70	62.20	11.10	Opaque glass

a glass/glass-ceramic transformation, and to investigate the crystallization kinetics of the glasses, non-isothermal differential thermal analysis curves were recorded in air at a heating rate of 20°C min⁻¹, using powdered specimens of about 35 mg. A Netzsch high-temperature DSC 404 thermoanalyser was used with an empty Pt crucible as reference material.

2.3. Heat treatments

Knowing the DTA curves and consequently the crystallization temperatures, some powdered glasses were subjected to controlled heat treatments. The heat treatments were conducted on a Pt plate, in a laboratory electric furnace at a heating rate of 20°C min⁻¹ to different temperatures and held isothermally for 1 h. After that, the specimens were extracted hot from the furnace and allowed to cool naturally to room temperature. Also, using the same conditions as before, bulk as-quenched glass samples were heat-treated.

2.4. X-ray diffraction

The amorphous nature of the as-quenched glasses and the crystalline phases developed during the heat treatments were investigated on thermally processed samples finely ground in an agate ball mill. The samples were analysed by a Philips PW 3710 computer-assisted X-ray (Cu K α) powder diffractometer (XRD) in the 2 θ range from 10° to 60°. Using a built-in computer search program, the X-ray diffraction patterns were matched to JCPDS data and corresponding crystalline phases in the glass-ceramics were identified.

2.5. Microscopic analysis

A scanning electron microscope (Philips model XL-40) was used to investigate the crystallization process. Sample surfaces were ground smooth, then polished with alumina paste. The polished samples were then coated with a thin Pd–Au film.

2.6. Calculation of the activation energy for crystallization

The DDTA method for surface crystallization (as suggested by Branda et al. [6] and Barbieri et al.) was applied to determine the activation energy for crystallization. Surface nucleation of glasses follows the relationships

$$E_m/R(1/T_{f_1} - 1/T_{f_2}) = C \quad (1)$$

where E_m is the activation energy (kJ mol^{-1}), R is the gas constant ($0.00832 \text{ kJ mol}^{-1} \text{ K}^{-1}$) and T_{f_1} and T_{f_2} (K) are respectively the DDTA peaks corresponding to the first and second inflection points of the DTA curve, as illustrated in Fig. 1. The factor C is a constant, and is equal to 1.59 when a surface nucleation mechanism is dominant.

3. Results and discussion

Table 1 shows the compositions of the seven glasses prepared in this work, which produce optically clear and bubble-free glasses.

3.1. Differential thermal analysis

The DTA curves for powdered samples of the as-quenched glasses studied are reported in Fig. 2. From an analysis of each DTA curve, it is possible to verify that the glass transition temperature (T_g), attributed to the first endothermic event, increases from 460 to 565°C as the ZrSiO_4 content increases. This behaviour is a consequence of

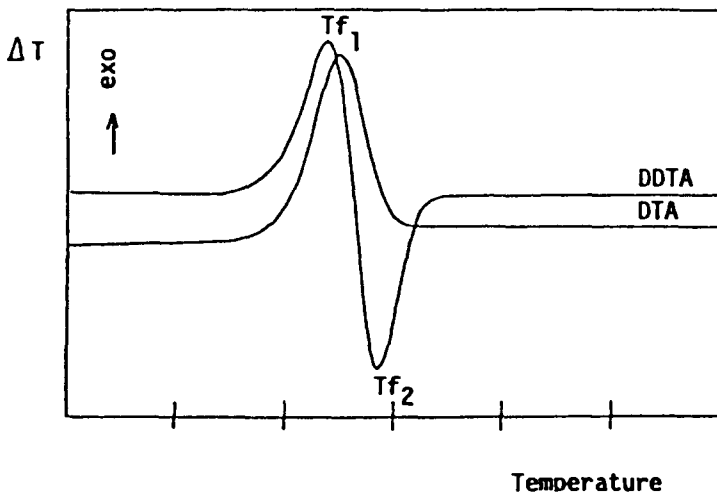


Fig. 1. Illustration of the DTA and DDTA curves related to the DDTA method for surface crystallization.

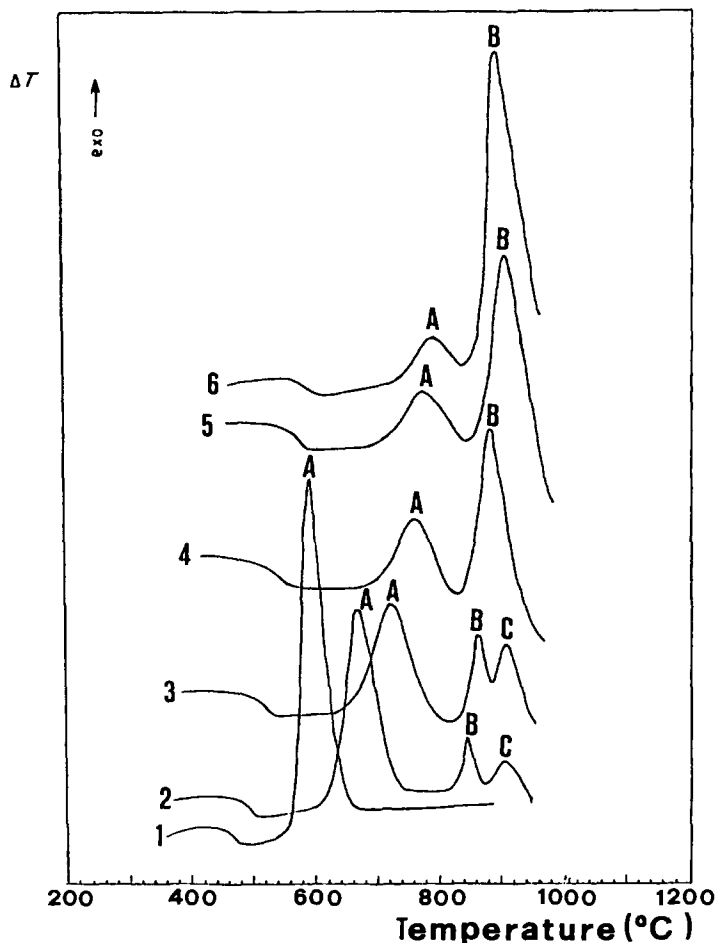


Fig. 2. DTA curves of the investigated glasses recorded at $20^{\circ}\text{C min}^{-1}$: 1, GC-0; 2, GC-1; 3, GC-2; 4, GC-3; 5, GC-4; 6, GC-5.

an increase in the glass viscosity, since the ZrO_2 is both an intermediate and a network glass-former [9–11]. Consequently, owing to the increase in bridging oxygen atoms per silicon atom, in the presence of Zr^{4+} glasses will result in a more packed structure with a higher T_g . Subsequently, exothermic events, indicating the development of crystallization (T_c), are observed for the glasses. The glass composition GC-0 (Fig. 2(1)) shows only one exothermic peak having a maximum rate of heat evolution at 590°C . However, when the ZrSiO_4 content increases up to 4.80 mol% and then from 7.00 to 10.30 mol%, three and two exothermic peaks are present respectively. This behaviour is typical of crystallized lithium silicate glasses, as reported by many authors [1–3, 10–12].

3.2. X-ray diffraction (XRD)

To determine the amorphous nature of the as-quenched glasses, glass samples of compositions GC-0 and GC-5 were analysed by X-ray diffraction; the patterns are shown in Figs. 3a, and b respectively. Both are characteristic of the glassy state. However, sample GC-6, see Fig. 3c, containing 11.10 mol% of ZrSiO_4 , shows peaks characteristic of crystalline zircon (ZrSiO_4) corresponding to SCPDS 6–266. Consequently, for zircon contents lower than 10.30 mol%, the results clearly indicate that it is possible to obtain completely amorphous glassy systems. For this reason, only the glasses from GC-0 to GC-5 were studied.

To identify the crystalline phases related to the exothermic events observed in the DTA curves, X-ray diffraction analysis was performed (Fig. 4) on some selected powdered samples GC-0, GC-1, GC-4 and GC-5, which exhibited the exothermic events. These samples were heat-treated to temperatures just above the exothermic event.

Glass composition GC-0: as-quenched powdered glass heat treated at 640°C for 1 h

This sample showed many reflections, see Fig. 4(a), indicating that the exothermic peak (A) is related to a crystallization process. The reflections can be assigned to a crystalline phase of lithium disilicate, $\text{Li}_2\text{Si}_2\text{O}_5$, JCPDS 24–651 and 30–767.

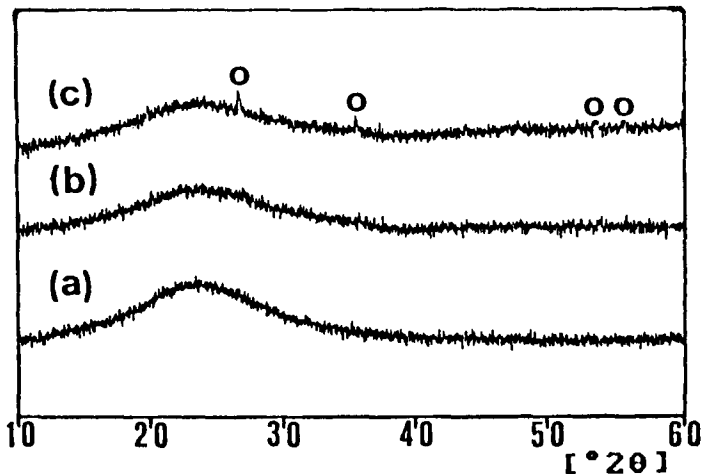


Fig. 3. X-ray diffraction patterns of samples: (a) as-quenched glass composition GC-0; (b) as-quenched glass composition GC-5 (10.30 mol% of ZrSiO_4); (c) additional as-quenched glass composition with 11.10 mol% of ZrSiO_4 ; o, zircon (ZrSiO_4).

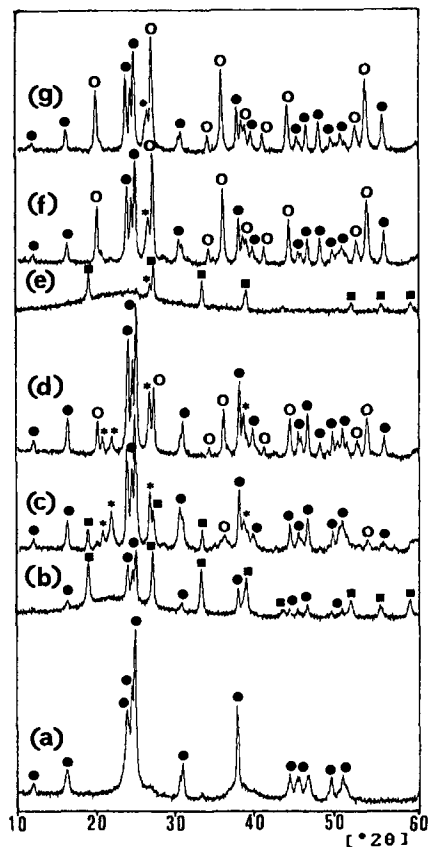


Fig. 4. X-ray diffraction patterns of samples: (a) glass composition GC-0 heat-treated at 640°C for 1 h; (b), (c), (d) glass composition GC-1 heat-treated at 750, 850 and 930°C for 1 h respectively; (e), (f) glass composition GC-4 heat-treated at 800 and 930°C for 1 h respectively; (g) glass composition GC-5 heat-treated at 900°C for 1 h; ●, lithium disilicate ($\text{Li}_2\text{Si}_2\text{O}_5$); ■, lithium metasilicate (Li_2SiO_3); ○, zircon (ZrSiO_4); *, tridymite.

Glass composition GC-1: as-quenched powdered glass heat treated at 750, 850 and 930°C for 1 h respectively

At 750°C, Fig. 4(b), the reflections of lithium disilicate ($\text{Li}_2\text{Si}_2\text{O}_5$) and lithium metasilicate, Li_2SiO_3 (JCPDS 29-828) appeared. In the sample heated to 850°C, Fig. 4(c), the intensity of the reflections related to the crystalline phase of Li_2SiO_3 decreased, whereas for the crystalline phase of $\text{Li}_2\text{Si}_2\text{O}_5$ it increased, with the appearance of the crystalline phases of ZrSiO_4 and tridymite (JCPDS 12-708, 14-260) in small amounts. However, at 930°C (Fig. 4(d)), the reflections related to the crystalline phase of Li_2SiO_3 disappeared, and those due to the crystalline phase of $\text{Li}_2\text{Si}_2\text{O}_5$, ZrSiO_4 and tridymite increased in intensity.

Glass composition GC-4: as-quenched powdered glass heat treated at 800 and 930°C for 1 h respectively

At 800°C, (Fig. 4(e)), the reflections of the crystalline phase of Li_2SiO_3 appeared, with low intensity reflections of tridymite. At 930°C, (Fig. 4(f)), the crystalline phase of Li_2SiO_3 disappeared. The spectrum indicates high amounts of crystalline phases of $\text{Li}_2\text{Si}_2\text{O}_5$ and ZrSiO_4 as well as the tridymite.

Glass composition GC-5: as-quenched powdered glass heat treated at 900°C for 1 h

In this case, the reflections (Fig. 4(g)) are the same as in the glass composition GC-4 at 930°C, and exhibit almost the same intensities.

4. Crystallization of glasses

4.1. Mechanism of crystallization

To investigate the mechanism of crystallization, bulk as-quenched glass samples for all the glass compositions were heat treated. With the exception of the glass composition GC-0, which was heat-treated at 640°C for 1 h, all other compositions were heat-treated at 930°C for 1 h. From SEM analysis of the heat-treated samples, a dominant surface mechanism of crystallization was observed, as shown in Fig. 5, corresponding to the glass composition GC-4. Only for the glass compositions GC-0, GC-1 and GC-2 does the mechanism seem to be a mix of surface and bulk crystallization. However, also for these compositions, if surface nucleation dominates, the kinetic analysis suggested in Section 2.6 is valid, for the fine powders employed in the DTA experiments.

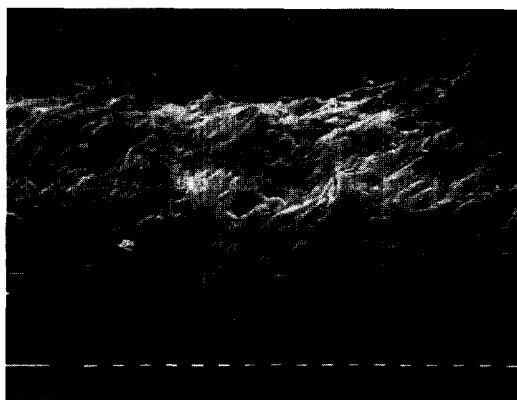


Fig. 5. SEM photomicrograph (320 X) of the GC-4 sample heat-treated at 930°C for 1 h.

4.2. Kinetics of crystallization

Table 2 shows the calculated activation energies for surface crystallization determined from Eq. (1), related to the exothermic events in the DTA curves, and the crystalline phases formed. As can be seen, the value of activation energy with respect to the first exothermic event peak (A) decreased by 50% when the ZrSiO_4 content was 2.40%, and then remained more or less constant up to 9.10 mol% of ZrSiO_4 but, tended to increase slightly when the ZrSiO_4 content reached 10.30 mol%. Consequently, a percentage of ZrSiO_4 of up to 4.80% lowers the activation energy progressively, while higher percentages do not exert any appreciable influence. This suggests a variation in the crystallization mechanism from lower to higher ZrSiO_4 contents. For the second exothermic event peak (B), the activation energy values behave in almost the same way as those for the first exothermic event peak (A). At the same time, the absolute values are about 3–4 times greater. For the last exothermic event, peak (C), when the ZrSiO_4 increases, the activation energy decreases. This decrease is also observed in the exothermic events related to the A and B peaks. However, the activation energies are lower than those related to the B peaks and higher than those for the A peaks.

Table 2
Activation energies and crystalline phases as a function of the chemical composition and the exothermic event involved

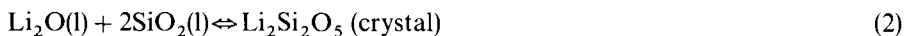
Glass compositions	Exothermic event A		Exothermic event B		Exothermic event C	
	$E_m/$ kJ mol^{-1}	Crystalline phases	$E_m/$ kJ mol^{-1}	Crystalline phases	$E_m/$ kJ mol^{-1}	Crystalline phases
GC-0	460.5	$\text{Li}_2\text{Si}_2\text{O}_5$	–	–	–	–
GC-1	230.3	$\text{Li}_2\text{Si}_2\text{O}_5$ Li_2SiO_3	958.8	$\text{Li}_2\text{Si}_2\text{O}_5$ ZrSiO_4 Li_2SiO_3 SiO_2^a	636.4	$\text{Li}_2\text{Si}_2\text{O}_5$ ZrSiO_4 SiO_2^a
GC-2	213.5	$\text{Li}_2\text{Si}_2\text{O}_5$ Li_2SiO_3	858.3	$\text{Li}_2\text{Si}_2\text{O}_5$ ZrSiO_4 Li_2SiO_3 SiO_2^a	573.6	$\text{Li}_2\text{Si}_2\text{O}_5$ ZrSiO_4 SiO_2^a
GC-3	226.1	Li_2SiO_3 SiO_2^a	548.5	$\text{Li}_2\text{Si}_2\text{O}_5$ ZrSiO_4 Li_2SiO_3 SiO_2^a	–	–
GC-4	221.9	Li_2SiO_3 SiO_2^a	519.2	$\text{Li}_2\text{Si}_2\text{O}_5$ ZrSiO_4 SiO_2^a	–	–
GC-5	263.8	Li_2SiO_3 SiO_2^a	715.9	$\text{Li}_2\text{Si}_2\text{O}_5$ ZrSiO_4 SiO_2^a	–	–

^a Tridymite.

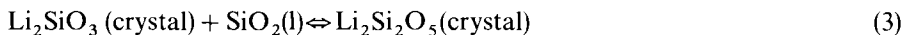
Combining all the experimental data and associating them with each exothermic event on the DTA curves, and following some theoretical considerations, the kinetics of crystallization can be explained as follows.

Exothermic event A

For the basic glass composition (GC-0), $\text{Li}_2\text{Si}_2\text{O}_5$ is the only crystalline phase obtained, in agreement with the $\text{Li}_2\text{O}-\text{SiO}_2$ phase diagram [2]. XRD and DTA evidence suggests that the reaction giving the lower temperature exothermic event (peak A) of Fig. 2(1) is



The crystallization of lithium disilicate ($\text{Li}_2\text{Si}_2\text{O}_5$), according to reaction (2), occurs at temperatures above 560°C and requires an activation energy of $460.5 \text{ kJ mol}^{-1}$. When the ZrSiO_4 content increases up to 4.80 mol%, both crystalline lithium metasilicate (Li_2SiO_3) and $\text{Li}_2\text{Si}_2\text{O}_5$ exist according to the equation

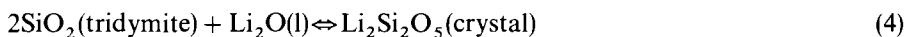


Subsequently, the amount of Li_2SiO_3 increases up to 7.00 mol% of ZrSiO_4 , when no $\text{Li}_2\text{Si}_2\text{O}_5$ is obtained. From 7.00 to 10.30 mol% of ZrSiO_4 , only Li_2SiO_3 and small amounts of tridymite are obtained. The observed rapid, preferential crystallization of lithium metasilicate (the kinetically favoured crystalline phase) can be explained by considering that the activation energy for its crystallization is much lower than that for lithium disilicate [12, 13]. In fact, a reduction of about 50% on the measured activation energy related to the crystallization of lithium metasilicate was observed experimentally. The slight increases of the activation energy observed from samples GC-2 to GC-5 can be accounted for by considering that the crystallization of lithium metasilicate removes equimolar quantities of Li_2O and SiO_2 from the molten glass, which increases the SiO_2 and ZrO_2 of the remaining glass, and increases its viscosity as well as its activation energy.

Exothermic event B

In this case, zircon (ZrSiO_4) and SiO_2 (tridymite) crystallize in the $845-906^\circ\text{C}$ temperature range for all the glass compositions containing ZrSiO_4 . The crystalline phases of $\text{Li}_2\text{Si}_2\text{O}_5$ and Li_2SiO_3 remain together with zircon and tridymite, up to 7.00 mol% of ZrSiO_4 . For ZrSiO_4 contents higher than 7.00 mol%, no Li_2SiO_3 exists, leaving only zircon, $\text{Li}_2\text{Si}_2\text{O}_5$ and tridymite. The formation of lithium disilicate can occur at expense of Li_2SiO_3 as described by reaction (3). However, the intensity of the X-ray diffraction reflections related to $\text{Li}_2\text{Si}_2\text{O}_5$ decreases when the ZrSiO_4 content in the glass increases, indicating an increase in the amount of zircon after crystallization. Recalling that tridymite, although only a small amount, had been crystallized in the exothermic event (A) for ZrSiO_4 contents higher than 7.00 mol%, a second mechanism of formation of $\text{Li}_2\text{Si}_2\text{O}_5$ may occur according to reaction (4) based on the mechanism

of $\text{Li}_2\text{Si}_2\text{O}_5$ crystallization from cristobalite [12]



Consequently, we can assume that for ZrSiO_4 contents between 2.40 and 4.80 mol%, the predominant mechanism seems to be that described by reaction (3), while for higher ZrSiO_4 contents, in addition to mechanism (3) the mechanism described by reaction (4) occurs and seems to be predominant.

Exothermic event C

This exothermic event occurs for ZrSiO_4 contents between 2.40 and 4.80 mol% (compositions GC-1 and GC-2). The crystalline phases zircon, $\text{Li}_2\text{Si}_2\text{O}_5$ and tridymite form in the 900–907°C temperature range. From the results, we may assume that the prevalent mechanism responsible for the lithium disilicate formation in these compositions is that described by reaction (3).

5. Conclusions

The glasses obtained by addition of ZrSiO_4 at 10.30 mol% to the $30\text{Li}_2\text{O}/70\text{SiO}_2$ composition are transparent and higher amounts of ZrSiO_4 are not completely solubilized. According to the structural theories of glass, the thermal properties of the composition $30\text{Li}_2\text{O}/70\text{SiO}_2$ are considerably modified by the addition of ZrSiO_4 from 0 to 10.30 mol%. Glass transition temperatures (T_g) ranging from 460 (base $30\text{Li}_2\text{O}/70\text{SiO}_2$ glass) to 565°C (glass with a ZrSiO_4 content of 10.30 mol%) were measured, due to the increase in bridging oxygen atoms per silicon atom. Glasses in the presence of Zr^{4+} will yield a more packed structure with a higher T_g .

Glass-ceramic materials characterized by a dominant surface crystallization mechanism, where the main crystalline phases are lithium disilicate ($\text{Li}_2\text{Si}_2\text{O}_5$), tridymite (SiO_2) and zircon (ZrSiO_4), can be obtained after a controlled devitrification process of all the compositions studied and containing ZrSiO_4 . The crystallization process occurs in one, two and three steps respectively, depending on the ZrSiO_4 addition, and the crystallization is completed in the 590–907°C temperature range. Lithium metasilicate (Li_2SiO_3) obtained during the exothermic event (A) completely transforms into lithium disilicate ($\text{Li}_2\text{Si}_2\text{O}_5$), and the addition of ZrSiO_4 as seeds, even at very low percentages, has a remarkably favourable effect on the crystallization of zircon with a lowering of the activation energy for higher ZrSiO_4 contents.

Finally, owing to the properties of the crystalline phases, the resulting materials have potential application as useful sintered glass-ceramics.

Acknowledgements

A.P.N. de Oliveira thanks the “Coordenação de Aperfeiçoamento de Pessoal de Nível Superior - CAPES and Federal University of Santa Catarina, both Brazilian

institutions, for financial support (scholarship) in pursuing his doctoral studies. The authors are also grateful to C.N.R. for financial support.

References

- [1] Z. Strnad, *Glass Science and Technology* 8, Elsevier, New York, 1986, p. 76–80.
- [2] A.R. West, *Solid State Chemistry and its Applications*, John Wiley and Sons, New York, 1984, p. 633–634.
- [3] M.H. Lewis, *Glasses and Glass-Ceramics*, Chapman and Hall, London, 1989, p. 23.
- [4] H. Simmons, D.R. Uhlmann and G.H. Beall, *Nucleation and Crystallization*, in *Glasses* 4, American Ceramic Society, USA, 1982, p. 146–152.
- [5] E. Ryshkewitch and D.W. Richerson, *Oxide Ceramics*, Academic Press, Florida, 1985, p. 350–397.
- [6] F. Branda, A. Buri, A. Marotta and S. Saiello, *J. Mater. Sci.*, 17 (1982) 105.
- [7] L. Barbieri, C. Leonelli, T. Manfredini, M. Paganelli and G.C. Pellacani, *J. Therm. Anal.* 38 (1992) 2639.
- [8] L. Barbieri, C. Leonelli, T. Manfredini, M. Romagnoli, G.C. Pellacani and C. Siligardi, *Thermochim. Acta*, 227 (1993) 125.
- [9] A.K. Varshneya, *Fundamentals of Inorganic Glasses*, Academic Press, New York, 1994, pp. 27–36, 183–208.
- [10] W.D. Kingery, H.K. Bowen and D.R. Uhlmann, *Introduction to Ceramics*, John Wiley and Sons, New York, 1960, p. 92–116.
- [11] D.R. Uhlmann and N.J. Kreidl, *Glass: Science and Technology* 1, Academic Press, New York, 1983, p. 1–4, 92–116.